Journal of Coastal Research	18	3	555–567	West Palm Beach, Florida	Summer 2002

T-S Data Assimilation to Optimise Turbulent Viscosity: An Application to the Berre Lagoon Hydrodynamics

Yann Leredde†, Ivan Dekeyser‡, and Jean-Luc Devenon§

†LOB, UMR 6535
Centre d'Océanologie de Marseille
Université de la Méditerranée
Campus de Luminy—Case 901
F 13288 Marseille Cedex 9, France
leredde@com.univ-mrs.fr

‡UMS 2196
Centre d'Océanologie de Marseille
Université de la Méditeranée
Campus de Luminy—Case 901
F 13288 Marseille Cedex 9, France
dekeyser@com.univ-mrs.fr

§LSEET
Université de Toulon et du Var
BP 132
F-83957 La Garde Cedex, France
devenon@lseet.univ-tnl.fr

ABSTRACT

LEREDDE, Y.; DEKEYSER, I., and DEVENON, J-L., 2002. T-S data assimilation to optimize turbulent viscosity: An application to the Berre lagoon hydrodynamics. *Journal of Coastal Research*, 18(3), 555–567. West Palm Beach (Florida), ISSN 0749-0208.

The Berre lagoon (France) is a semi-enclosed basin with 6 m of mean depth and 155 km^2 of surface area. Due to the Durance river discharge in the north and the Mediterranean sea intrusion in the south, the hydrological situation is often strongly stratified. The vertical mixing occurs only when high wind is blowing (> 10ms^{-1}).

Modelling the basin circulation during such a process with a 3-D primitive equation model requires an accurate parameterisation of the turbulent vertical viscosity and diffusivities. A classical approach consists in using a turbulence model like the k-L or k-ϵ ones. Here, an alternative approach is to consider the vertical turbulent viscosity ν_t as a space and time dependent function to be fitted, under the assumption of constant Prandtl and Schmidt coefficients for the turbulent diffusivities. ν_t is optimised, iteratively, for each vertical level and with a period of half an hour, in order to minimise the discrepancies between the simulation results and the salinity and temperature data profiles measured by a measurement station at the same time rate. This iterative procedure requires to solve an adjoint model to assimilate the data.

This optimal control method is applied on a 3-days wind event and gives simulation results closer to the data than could be expected when using a classical k + L model without data assimilation.

ADDITIONAL INDEX WORDS: *Turbulent viscosity, optimal control, adjoint model, data assimilation, Berre lagoon.*

INTRODUCTION

Located in the most industrialised and populated region of the French Mediterranean littoral (Figure 1), the Berre lagoon is its broadest salty lagoon with a surface area of 155 km^2. It has a mean depth of 6 m and a maximum depth of 9 m (see the bathymetry on Figure 1). This lagoon is often considered as a polluted area because of a long period of industrial and urban sewage badly controlled in the past. In fact, the hydrological situation is complexified by massive inputs of fresh water on the one hand and marine water on the other hand. At the beginning of the 20th century, the Caronte canal, linking the lagoon at its Southwest to the Mediterranean sea, was deepened. The lagoon had then the same hydrological and biological properties than the sea. Since 1966, a part of the Durance river water has been channelled to an hydroelectric power plant, located in Saint Chamas at the north of the basin. Irregular quantities of fresh water are discharged with a mean flow of 85 m^{3}s^{-1}. These fresh water inputs induce a strong vertical stratification. The sharp pycnocline, located between 3 and 7 m depth following the season, acts as a wall for the gaze exchanges. Important ecological problems are then induced by the anoxia of the lower layer (SCHILTZ *et al.*, 2001).

The stratified situation is very stable and only strong gusts of wind (> 10ms^{-1}) allow the mixing of the water masses. These strong winds mainly blow from North-Northwest and are called Mistral. This physical process has a great importance on the ecological situation and this is why the hydrodynamics of the Berre lagoon is here studied.

In order to succeed in this task, we had the opportunity to use hydrological data measured by a measurement station set up in the centre of the basin (NERINI *et al.*, 2000). The physical parameters of temperature and salinity are measured every half an hour at 1, 2, 4, 6 and 8 m depths. Meteorological data, taken every 3-h at the Marseilles airport station, are also available. These data give first information on a strong wind response of the basin.

Nevertheless, as it can be done today, a 3-D primitive equation model (LEENDERTSE *et al.*, 1973) is used to simulate the basin hydrodynamic circulation during such a wind event.

In this kind of hydrodynamic model, the system of partial differential equations to be solved for mean momentum, heat and salt is not closed and a classical way is to use a turbu-

00010 received 25 July 2000; accepted in revision 10 November 2001.

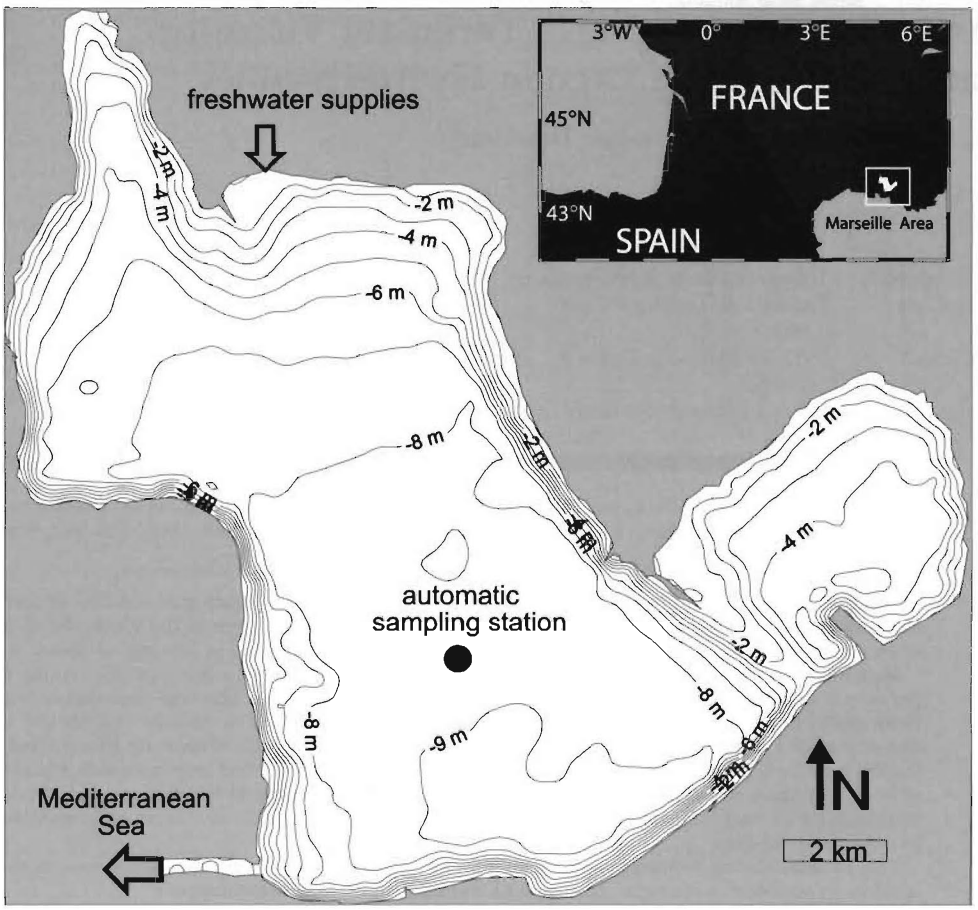

Figure 1. Location map and bathymetry of the Berre lagoon (from NERINI *et al.*, 2000).

lence model (MELLOR and YAMADA, 1982). In a first attempt, a k+L formulation, with a single transport equation for the kinetic turbulent energy k and an empirical mixing length scale L, have been developed and tested (LEENDERTSE and LIU, 1977; LEREDDE, 1999).

As an alternative to this direct approach, an inverse strategy has been proposed to estimate the turbulent viscosity and diffusivity from oceanographic observations (LEREDDE *et al.*, 1999). The method is a specific case of the optimal control method often called the adjoint method (SEILER, 1993). The ideas and mathematical concepts of optimal control theory were formalised about thirty years ago (LIONS, 1968) and have since received much attention for applications in oceanography (BEGIS and CREPON, 1975; DEVENON, 1990). The aim of the optimal control method is to find the best parameters of a model to simulate the computed values closest to those observed. The adjoint method has been most often used to fit initial conditions (MOORE, 1991), but also boundary conditions (LELLOUCHE *et al.*, 1998), or specific parameters (ROQUET *et al.*, 1993). This variational method involves the minimisation of a cost function which is the norm of the difference between the computed and observed values. An algorithm is obtained via the so-called adjoint equations for the construction of the gradient of the cost function with respect to the parameters. Once the gradient has been determined, the minimisation can be performed using any gradient descent algorithm.

The efficiency of the optimal control method to optimise time-constant viscosity distributions in 1-D vertical models has already been underlined (YU and O'BRIEN, 1991; PANCHANG and RICHARDSON, 1993; EKNES and EVENSEN, 1997). In a more recent study, a 3-D primitive equation model has been adopted (LEREDDE *et al.*, 1999). The model and its full turbulence formulation (k+L) was used to simulate synthetic observations (velocity, salinity or temperature) of two wind driven events: the first concerns an open stratified ocean, and the second, a coastal upwelling. These data were assimilated to reconstruct the turbulent viscosity field, which depends either on time and 1-D space or 2-D space. The adjoint model of the direct model (without the complete turbulence formulation) is integrated backward in time to compute the gradient of the cost function with respect to the control and therefore performs the minimisation. This study showed the interest and above all the feasibility of the method. Today, this method, efficient on schematic situations, must be applied to concrete geophysical problems. Typically in the past, the

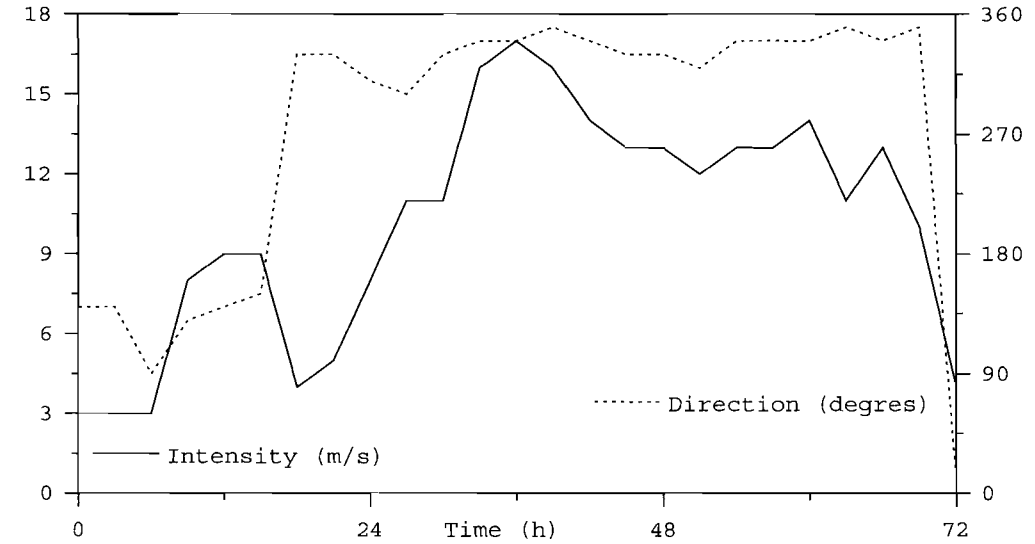

Figure 2. Wind data from June 21, 1996, 00 h, every 3h at the weather station of the Marignane airport. Dotted line and right axis: direction in degrees (clockwise from the North). Solid line and left axis: wind velocity in ms $^{-1}$.

mean problems encountered in this kind of applications on real oceanographic situations are due to the difficulties to collect data of sufficient quantity and quality in the oceanic domain. It makes no doubt that the atmospheric observations have a more favourable nature and so that the variational methods are today much more used in meteorology than in oceanography (*e.g.* LE DIMET and TALAGRAND, 1986).

The present study can be seen as one of the first example of the efficiency of variational methods in order to answer concrete coastal oceanographic problems. The Berre lagoon hydrodynamics and the corresponding hydrological data allow to make this demonstration.

In a first section, hydrological data are presented and analysed in order to give first interpretations but also to arise questions about a typical event of wind and mixing. In a second section, the 3D primitive model and its full direct turbulence formulation is described and used to simulate the previously described physical event. This direct simulation work is similar to the one of BLUMBERG and GOODRICH (1990) who have simulated, with the k-kL model of MELLOR and YAMADA (1982), the destratification effect induced by the wind in the Chesapeake bay. In the third section, the optimal control formalism is briefly recalled and applied. As an alternative to a direct simulation with the k+L model, the data are assimilated in order to optimise the turbulent viscosity of a zero order model and to obtain the closest simulation to the data. Discussions and conclusions are presented in a last section.

The Data

The three-day period, corresponding to a north-westerly wind event (Mistral), in June 1996, is a classical meteorological episode in this region. The wind data (Figure 2) were acquired every 3 hours from the meteorological station of Marignane airport, near the east side of the basin. A two-day Mistral period follows a rather calm period of southeast wind. The salinity and temperature data (Figure 3) are available every 30 minutes at the automatic measurement station at depths 1, 2, 4, 6 and 8 m. Even if the measurement station provides a partial view of the basin answer to wind forcing, it helps us to understand the acting physical processes. At the beginning of the period (06/21 at 00 h), the Berre lagoon at the measurement station location is strongly stratified both in salinity and temperature. The surface layer (1 to 4 m) is much less dense (σ = 6, S = 12, T = 25°C) than the deepest layer at 8 m (σ = 22, S = 30, T = 17°C). The 6-m depth sensor provides intermediate values (σ = 11, S = 17, T = 19°C). One can notice that the salinity value at 1-m depth seems rather biased considering that it is higher than the ones at 2 and 4 m depth during all the studied period, and so leading to a density anomaly corresponding to an unstable stratification state.

As long as the wind is weak, the stratified situation remains stable. The stronger wind, blowing since the 06/22 at 0h, then tends to homogenise the entire water column, but with a threshold and some delay (12 h) after the beginning of the gust of wind. In order to understand this delay and this sudden mixing event (nearly at t = 36 h), one can go back to the results obtained in a 1D schematic case (LEREDDE *et al.,* 1999). The wind induces a mixing in the upper layer of the water column. The turbulent energy remains trapped in this fresh upper layer until mechanical mixing energy, resulting from the downward diffusion of a fraction of the wind energy input, overcomes the stabilising effect of the stratification. Then, the pycnocline is suddenly broken, the motion and the heat can diffuse downward and the salinity upward.

Nevertheless, by contrary to the 1D schematic case studied by LEREDDE *et al.* (1999), the vertical diffusion is not the only

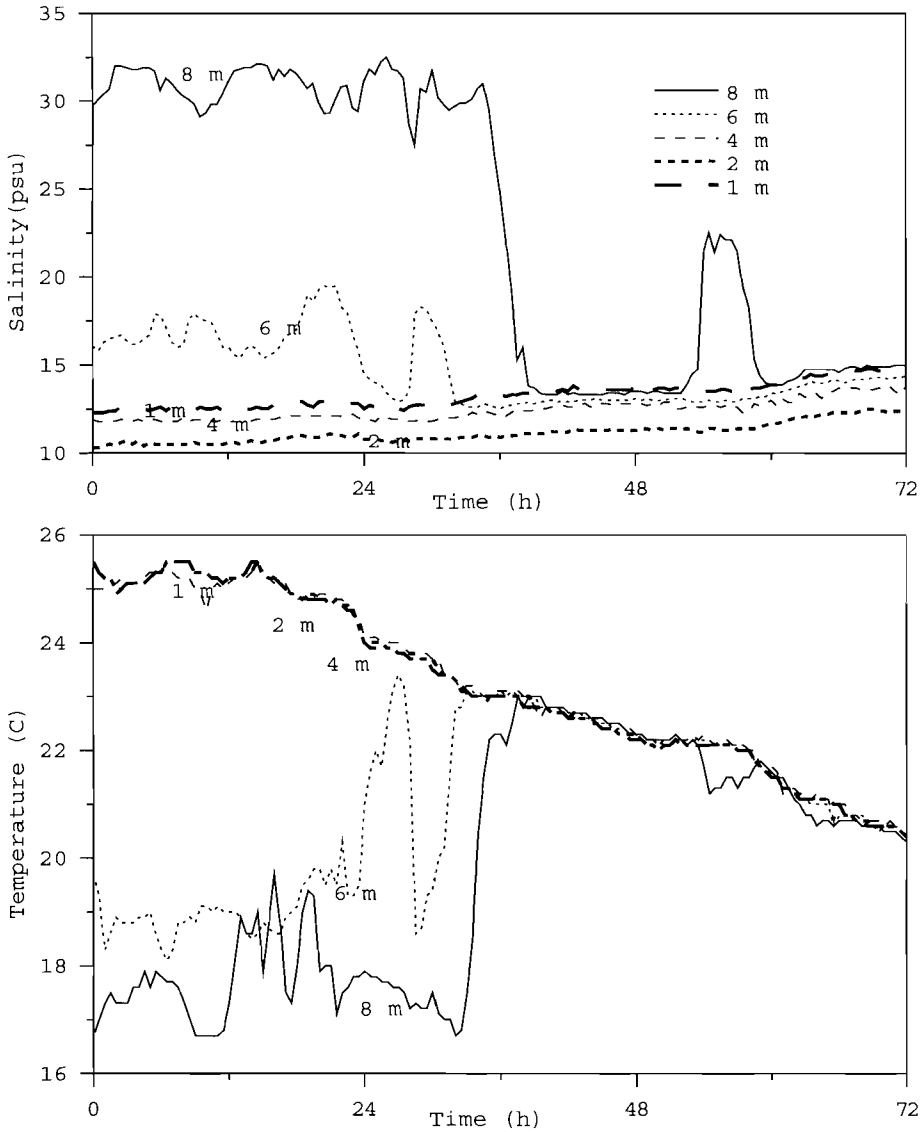

Figure 3. Salinity and temperature at the measurement station. Data every 30 mn on 5 sensors (1, 2, 4, 6, 8 m depths).

process involved here. For example, the restratificaiton episode between t = 54 h and t = 60 h, revealed by the 8-m deep sensor of salinity and temperature, cannot be explained by the vertical diffusion process only. The first-step towards a realistic explanation would be to invoke an advection of a salty and colder water from elsewhere.

The Direct Simulation with the k+L Model

The Direct Model

The direct model (LEENDERTSE *et al.*, 1973), recently reimplemented (LELLOUCHE, 1995) is a classical primitive equation model for coastal seas. Many others are based on a similar approach (*e.g.* NIHOUL, 1977; THOUVENIN and SALOMON, 1984; VAN DAM and LOUWERSHEIMER, 1990). The Boussinesq approximation (constant density except in the buoyancy term), and those of hydrostasy and f-plane are made. The physical state of the fluid is given by the seven following equations for the average variables.

$$\frac{\partial u}{\partial t} + \frac{\partial (uu)}{\partial x} + \frac{\partial (uv)}{\partial y} + \frac{\partial (uw)}{\partial z} - fv + \frac{1}{\rho_0}\frac{\partial p}{\partial x} - \frac{\nu_h}{\rho_0}\left(\frac{\partial^2 u}{\partial x^2} + \frac{\partial^2 u}{\partial y^2}\right) - \frac{1}{\rho_0}\left(\frac{\partial}{\partial z}\left(\nu_t \frac{\partial u}{\partial z}\right)\right) = 0 \quad (1)$$

$$\frac{\partial v}{\partial t} + \frac{\partial (vu)}{\partial x} + \frac{\partial (vv)}{\partial y} + \frac{\partial (vw)}{\partial z} + fu + \frac{1}{\rho_0}\frac{\partial p}{\partial y} - \frac{\nu_h}{\rho_0}\left(\frac{\partial^2 v}{\partial x^2} + \frac{\partial^2 v}{\partial y^2}\right) - \frac{1}{\rho_0}\left(\frac{\partial}{\partial z}\left(\nu_t \frac{\partial v}{\partial z}\right)\right) = 0 \quad (2)$$

$$\frac{\partial p}{\partial z} = -\rho g \tag{3}$$

$$\frac{\partial u}{\partial x} + \frac{\partial v}{\partial y} + \frac{\partial w}{\partial z} = 0 \tag{4}$$

$$\frac{\partial S}{\partial t} + \frac{\partial (uS)}{\partial x} + \frac{\partial (vS)}{\partial y} + \frac{\partial (wS)}{\partial z} - \nu_h^S \left(\frac{\partial^2 S}{\partial x^2} + \frac{\partial^2 S}{\partial y^2} \right) - \frac{\partial}{\partial z} \left(\nu_t^S \frac{\partial S}{\partial z} \right) = 0 \tag{5}$$

$$\frac{\partial T}{\partial t} + \frac{\partial (uT)}{\partial x} + \frac{\partial (vT)}{\partial y} + \frac{\partial (wT)}{\partial z} - \nu_h^T \left(\frac{\partial^2 T}{\partial x^2} = \frac{\partial^2 T}{\partial y^2} \right) - \frac{\partial}{\partial z} \left(\nu_t^T \frac{\partial T}{\partial z} \right) = 0 \tag{6}$$

$$\rho = \rho_0 (1 + \alpha_S (S - S_0) + \alpha_T (T - T_0)) \tag{7}$$

In this set of equations, u, v, w are the mean velocity components in the three space dimensions x (East), y (North), z (Zenith); t denotes the time, p the pressure, S the salinity, T the temperature, ρ the sea-water density. ρ_0, T_0, S_0 are constant reference values for density, temperature and salinity. f is the Coriolis parameter, g the gravitational acceleration, α_S the saline contraction coefficient, α_T the volumetric expansion coefficient.

The turbulent shear stresses, the turbulent heat and salinity fluxes are computed by use of eddy-viscosity and eddy-diffusivity concepts and the molecular effects are neglected.

A first approach, the zero order turbulence closure, consists in giving constant values to the horizontal and vertical turbulent viscosity coefficients (ν_h and ν_t) and to the horizontal (ν_h^T and ν_h^S) and vertical (ν_t^T and ν_t^S) turbulent diffusivity coefficients, without using additional transport equations.

At the upper boundary, the horizontal wind stress vector $\vec{\tau}$ can be estimated by the quadratic expression:

$$\vec{\tau} = C_d \rho_a \|\vec{U}_w\| \vec{U}_w \tag{8}$$

where ρ_a is the air density, $\vec{U}_w$ the wind speed vector at 10 metres above mean sea surface and a drag coefficient $C_d = 2.5 \times 10^{-3}$.

The bottom stress vector $\vec{\tau}_b$ is also expressed in the same way:

$$\vec{\tau}_b = \rho_b g \frac{\|\vec{U}_b\| \vec{U}_b}{C^2} \tag{9}$$

where ρ_b is the water density at the bottom layer, $\vec{U}_b$ is the horizontal velocity vector at the bottom layer and the square of the Chezy coefficient $C^2 = 4.10^4$ ms^{-2}.

For the numerical implementation (LELLOUCHE, 1995), a finite difference approximation has been used both in time and space according to a vertical multilevel geometrical discretisation.

In a first version of the model, used for open boundary condition optimisation (LELLOUCHE *et al.*, 1998), the turbulent viscosity and diffusivity coefficients were all set to constant values. A simple study of sensitivity of the model to the horizontal viscosity and diffusivity coefficients values shows that the horizontal diffusion terms are helpful to damp down the small scale instabilities. Nevertheless a first approximation given by constant horizontal coefficients seems to be sufficient.

In contrast, the vertical turbulent viscosity and diffusivity have a real influence, particularly in the case of stratified seas, and must be specified with more accuracy.

A classical approach consists in using a turbulence model expressing the turbulent viscosity and diffusivity coefficients as functions of the turbulent state of the sea water. In the framework of this study and in order to progress towards our assimilation aims, a k-model, initially developed by LEENDERTSE and LIU (1977), has been chosen. In this model, called hereafter the k+L model, the vertical eddy viscosity coefficient ν_t is evaluated by using a buoyancy extended Prandtl-Kolmogorov hypothesis.

$$\nu_t = C_\nu \sqrt{k} L \exp(-mRi) \tag{10}$$

where L is a mixing length scale given by an algebraic parabolic function of the distance to the surface, k the turbulent kinetic energy, Ri is a "turbulent" Richardson number and m and C_ν two positive constants, respectively equal to 0.01 and 0.09.

The vertical eddy diffusivities for heat and salt transport are assumed to be equal to the turbulent vertical viscosity via respectively turbulent Prandtl and Schmidt numbers equal to 1.

The turbulent kinetic energy is governed by a classical transport equation including shear and buoyant production terms and a dissipation term. There is no flux of turbulent kinetic energy at the boundaries.

For sake of synthesis, the detailed equations are not presented here but can be found in LEREDDE *et al.* (1999). This model, in its revised form, has been validated and calibrated for various classical coastal configurations (LEREDDE, 1999). It was mainly developed to test the feasibility of the data assimilation method of optimal control and used to progress towards numerical aims. In the present study, this simple model is used to simulate a real observed situation.

Direct Experiment

The Berre lagoon is included in a parallelepiped volume of 20 km by 20 km at the horizontal and 9 m at the vertical. In order to keep a reasonable numerical cost, a rather crude grid is adopted. The horizontal mesh size is 1000 m and the vertical (z) one is 1 m. The bathymetry is approximated by step stairs to nearest to the real bathymetry (Figure 1). The associated time step, based on the numerical CFL stability criteria is 10 s.

The success of the simulation experiment is not only controlled by the vertical turbulent viscosity distribution. As in any simulation experiment, the specification and the accuracy of the initial and boundary conditions, which are other model control parameters, are required to determine the solution.

In addition to the station measurements, episodic and sparse T-S observations (10 sampling points every 15 to 20 days) have been carried out. These data cannot be used directly to specify hydrological initial conditions. However they

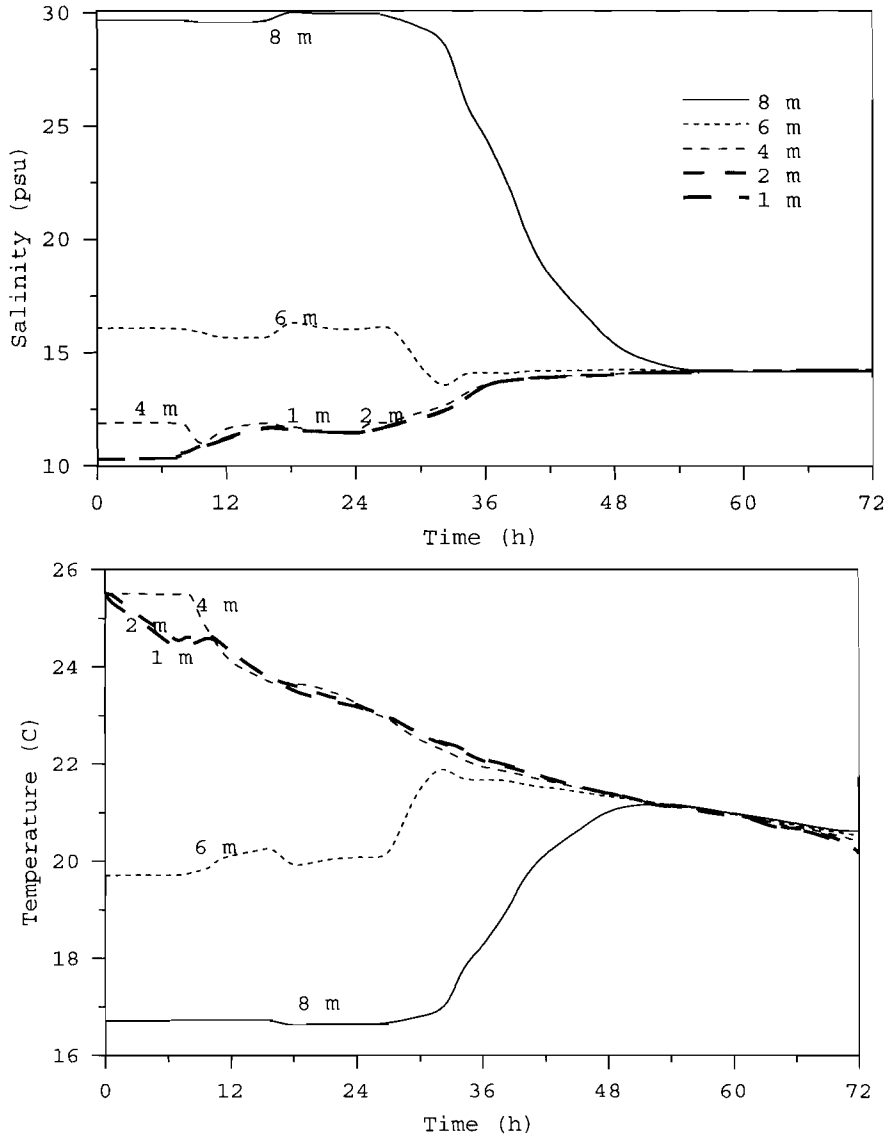

Figure 4. Salinity and temperature simulated by the k+L model at the measurement station.

give a rough idea of the space variability of the stratification (NERINI *et al.*, 2001). When the wind speed is weak ($< 5 ms^{-1}$), the stratification is almost the same in all the basin except near the Saint Chamas power plant discharge or near the Caronte channel input (Figure 1). Before the starting day of the simulation (06/21/96) the wind was weak. So, the salinity and temperature data provided by the measurement station at the beginning of the period have been extended to the entire basin and considered as initial conditions. The initial dynamic conditions remain unknown, but the initial atmospheric state being calm, a state at rest of the lagoon and a zero free surface elevation are assumed at the initial time.

The Berre lagoon is almost closed, except the openings of Caronte and Saint Chamas. Apart from a local influence, these openings have a longer-term role than the action of a strong gust of wind on the hydrodynamics of the basin. For longer simulation experiments and to study the phenomena of stratification, there is no doubt that it would be necessary to take these contributions into account. In order to simplify, the effects of these openings will be neglected for the duration of the three days experiment. No-slip conditions are applied to the solid lateral boundaries of the domain. As no surface thermal fluxes were available, a constant cooling rate Q has been used to account for the temperature decrease. So, for the surface layer, an additional term $-(Q)/(\rho_0 c_p)$ with c_p the specific heat is added to equation (6).

The simulation results of the k+L model at the location of the station (Figure 4) can be compared to the observations (Figure 3). The general behaviours of the temperature and salinity distributions are almost reproduced. A threshold pro-

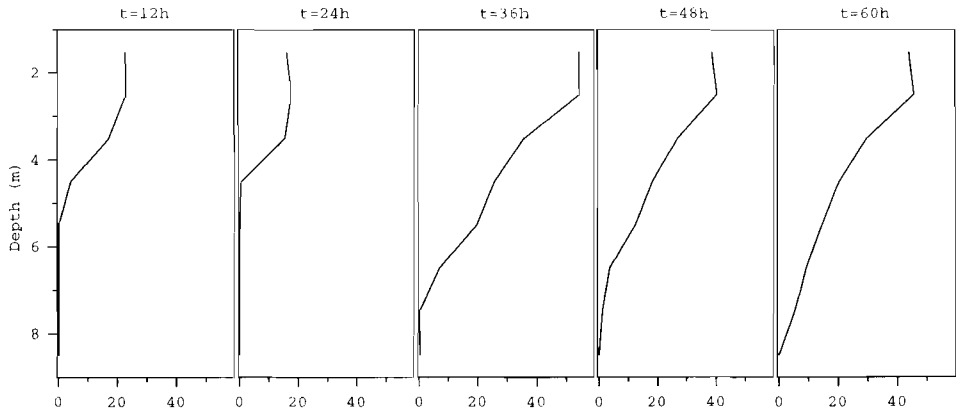

Figure 5. Vertical profiles of turbulent viscosity (cm^2s^{-1}) simulated by the k+L model at the measurement station.

cess of mixing is predicted but it is however less abrupt than the observed one. The release of the mixing process at the right time is not so good. The observed data show that the threshold process of mixing of the layer at 8 m depth occurs at t = 36 h. The turbulent viscosity computed by the k+L model (Figure 5) increases with the mechanical mixing energy input by wind but the pycnoclyne breaking is too smooth and the mixing is extended until almost t = 60 h.

The stratification episode from t = 54 h to t = 60 h is no more recovered. This feature will be discussed in details further (section 4.2). In the same way, because of the rather crude grid but probably also due to physical processes (KH instabilities, billows, internal waves breakings) which are not reachable to the actual hydrostatic model, the high-frequency variability of the *in-situ* measurements cannot be reproduced. They certainly play a rather important role in the layers mixing. The information brought by the data through assimilation will allow to take their effect into account via the turbulent viscosity fitting.

Though it would be possible to improve this numerical simulation by grid refinement, better suited initial or/and boundary conditions, higher turbulence closure, the choice made here corresponds to another point of view. Our aim is to show that a real data variational assimilation method is sufficient in it-self to produce accurate results. Indeed, this alternative approach is possible because of the existence of the linear tangent adjoint model of the retained version of the Leendertse code (LELLOUCHE *et al.*, 1998).

Assimilation Experiment

The Optimal Control Methodology

The method developed hereafter is adapted from LEREDDE *et al.* (1999). Each 30 minutes sequence between two temperature and salinity measured profiles, the aim is to find the optimal turbulent viscosity and diffusivities fields which allow the closest simulation results to the observations at the end of the sequence.

In order to keep the optimisation problem over-determined or, at least, well determined, the turbulent viscosity (ν_t) is imposed to be horizontally uniform and only depth and time dependent with a constant value for each 30-min sequence. Moreover, the turbulent diffusiviies for the temperature and the salinity are considered to be equal to the turbulent viscosity ($Pr = Sc = 1$). For each sequence, we chose to minimise the cost function

$$J = \frac{1}{2H}\int_{-H}^{0}\left[\frac{(T_f(z) - \hat{T}_f(z))^2}{\sigma^2_{\hat{T}_f}} + \frac{(S_f(z) - \hat{S}_f(z))^2}{\sigma^2_{\hat{S}_f}}\right]dz + \frac{1}{2H}\int_{-H}^{0} W_{\nu_t^b}(\nu_t(z) - \nu_t^b(z))^2\,dz \quad (11)$$

$T_f(z)$ and $S_f(z)$ are the temperature and salinity profiles simulated at the location of the measurement station, at the end of the considered sequence. $\hat{T}_f(z)$ and $\hat{S}_f(z)$ are the observed profiles at the end of the sequence $\sigma^2_{\hat{T}_f}$ and $\sigma^2_{\hat{S}_f}$ are their corresponding error variances. The background $\nu_t^b(z)$ is the optimal profile obtained for the previous sequence. For the first sequence, $\nu_t^b(z)$ is arbitrarily fixed at 10 cm^2s^{-1}. The first term expresses the discrepancies between the simulation results and the observations at the end of the sequence. The second term, so-called the regularisation term, is used to ensure that the optimal control is unique and not too far from the first guess $\nu_t^b(z)$. $W_{\nu_t^b}$ allows to choose the relative weight of the second term. This term improves the convergence of the minimisation method (YU and O'BRIEN, 1991; PANGHANG and RICHARDSON, 1993) and allows a temporal continuity of the optimal viscosity profiles. A classical way to minimise the cost function with respect to ν_t consists in computing its gradient $\nabla J(Y(\nu_t))$ and in using it in a quasi Newton algorithm (GILBERT and LEMARECHAL, 1989). Introducing the adjoint variables $u^*, v^*, w^*, p^*, S^*, T^*, \rho^*$ which verify the adjoint equations

$$\frac{\partial u^*}{\partial t} + 2u\frac{\partial u^*}{\partial x} + v\left(\frac{\partial u^*}{\partial y} + \frac{\partial v^*}{\partial x}\right) + w\frac{\partial u^*}{\partial z} - fv^* + S\frac{\partial S^*}{\partial x} + T\frac{\partial T^*}{\partial x} + \frac{\nu_h}{\rho_0}\left[\frac{\partial^2 u^*}{\partial x^2} + \frac{\partial^2 u^*}{\partial y^2}\right] + \frac{1}{\rho_0}\left[\frac{\partial}{\partial z}\left(\nu_t\frac{\partial u^*}{\partial z}\right)\right] = 0 \quad (12)$$

$$\frac{\partial v^*}{\partial t} + 2v\frac{\partial v^*}{\partial y} + u\left(\frac{\partial v^*}{\partial x} + \frac{\partial u^*}{\partial y}\right) + w\frac{\partial v^*}{\partial z} + fu^* + S\frac{\partial S^*}{\partial y} + T\frac{\partial T^*}{\partial y} + \frac{\nu_h}{\rho_0}\left[\frac{\partial^2 v^*}{\partial x^2} + \frac{\partial^2 v^*}{\partial y^2}\right] + \frac{1}{\rho_0}\left[\frac{\partial}{\partial z}\left(\nu_t\frac{\partial v^*}{\partial z}\right)\right] = 0 \quad (13)$$

$$\frac{\partial p^*}{\partial z} - \frac{1}{\rho_0}\left(\frac{\partial u^*}{\partial x} + \frac{\partial v^*}{\partial y}\right) = 0 \quad (14)$$

$$\frac{\partial w^*}{\partial z} + u\frac{\partial u^*}{\partial z} + v\frac{\partial v^*}{\partial z} + S\frac{\partial S^*}{\partial z} + T\frac{\partial T^*}{\partial z} = 0 \quad (15)$$

$$\frac{\partial S^*}{\partial t} + u\frac{\partial S^*}{\partial x} + v\frac{\partial S^*}{\partial y} + w\frac{\partial S^*}{\partial z} + \rho_0\alpha_S\rho^* + \nu_h^S\left[\frac{\partial^2 S^*}{\partial x^2} + \frac{\partial^2 S^*}{\partial y^2}\right] + \left[\frac{\partial}{\partial z}\left(\nu_t^S\frac{\partial S^*}{\partial z}\right)\right] = \frac{S - \hat{S}}{\sigma_S^2} \quad (16)$$

$$\frac{\partial T^*}{\partial t} + u\frac{\partial T^*}{\partial x} + v\frac{\partial T^*}{\partial y} + w\frac{\partial T^*}{\partial z} + \rho_0\alpha_T\rho^* + \nu_h^T\left[\frac{\partial^2 T^*}{\partial x^2} + \frac{\partial^2 T^*}{\partial y^2}\right] + \left[\frac{\partial}{\partial z}\left(\nu_t^T\frac{\partial T^*}{\partial z}\right)\right] = \frac{T - \hat{T}}{\sigma_T^2} \quad (17)$$

$$\rho^* + gp^* = 0 \quad (18)$$

it can be shown (LEREDDE *et al.*, 1999) that the expression of the gradient is given by:

$$\nabla J(Y(\nu_t(z))) = \frac{1}{\Omega}\frac{1}{\tau}\int_\Omega\int_0^\tau\left[\frac{1}{\rho_0}\frac{\partial u}{\partial z}\frac{\partial u^*}{\partial z} + \frac{1}{\rho_0}\frac{\partial v}{\partial z}\frac{\partial v^*}{\partial z} + \frac{\partial S}{\partial z}\frac{\partial S^*}{\partial z} + \frac{\partial T}{\partial z}\frac{\partial T^*}{\partial z}\right]d\Omega\, d\tau \quad (19)$$

τ is the duration of a sequence (τ = 30 min) and Ω is the horizontal domain. Except at the location of the station, there is no observations $\hat{T}$ and $\hat{S}$. As usual, when observations are not available, their error variances $\sigma_{\hat{T}}^2$ and $\sigma_{\hat{S}}^2$ are set to very large values to account for this lack of information. Consequently, the right hand terms of equations (16) and (17) are also null, except at the location of the measurement station.

For the numerical implementation, this continuous formulation must be converted to a discretised one. The way to proceed is not straightforward and involves theoretical and technical developments (LELLOUCHE *et al.*, 1998, LEREDDE *et al.*, 1998). Otherwise, it can be noticed that another way to obtain an adjoint code consists in using the automatic differentiation method directly from the source code (MAROTZKE *et al.*, 1999).

The vertical turbulent viscosity profile is optimised for a single sequence integrating iteratively forward in time the direct model and backward in time the adjoint model for this only sequence. The vertical discretisation induces that the vertical profile of ν_t and the discretised gradient of J are represented by 8 vector components. For each sequence, the optimisation problem has a weak dimension, the first guess is consistent and the method converges quickly for each sequence (between 2 and 10 iterations). Once the eddy viscosity of the sequence is optimised, the final simulation results are considered as the optimal solution and used to initialise the following sequence.

Numerical Results

The comparison of the simulation results at the station location (Figure 6) with the *in-situ* data (Figure 3) shows the efficiency of the method to reproduce the data with good accuracy. The high frequency variability is recovered and the mixing threshold process of the 6 m and 8 m layers is well reproduced.

It can also be noticed that the stratification episode observed around t = 60 h at 8 m depth is retrieved. A better understanding of the concerned physical process is now possible.

In the direct simulation without data assimilation the southward and near bottom saltier and colder water mass featured by the 9 m depth layer is nearly not mixed with the immediate upper layer. The vertical turbulent viscosity at 8.5 m depth, which drives the mixing between the 8 and 9 m layers, remains quite low (< 0.4 cm^{2}s^{-1}), even when the wind energy input is maximum (at t = 36 h). As shown in Figure 7, the velocity remains close to zero and this water mass is neither no more advected. Without either mixing or advection of this water mass, the observed stratification episode is not recovered by the direct simulation.

On the contrary, the data assimilation method permits to reproduce it, as the optimised vertical turbulent viscosity at 8.5 m depth (around 10 cm^{2}s^{-1}, see Figure 8) allows the vertical mixing of the 8 and 9 m layers from t = 54 h. Note that the horizontal advection process working alone is unable to produce the stratification episode. Indeed, the observed salinity (22) for the 8 m layer at t = 56 h implies the contribution of the mixing process without which salinity values would be higher (between 30 and 39). It is no more the result of a single vertical mixing process for the obvious reason that the salinity observed at 8 m depth at t = 60 h returns back to the values observed before t = 54 h. The fitting of the turbulent coefficients via the data assimilation method permits to reproduce such an advecto-diffusive process initially missing in the direct simulation results.

However, at first glance, other subtle effects could be invoked. For instance, it is quite obvious that a more salted water stocked in the deepest layer of the lagoon could provide other optimised turbulent diffusivity coefficients. Indeed, the saltier it is, the weaker the diffusion will be. Nevertheless, salinity exceeding 39 cannot be envisaged for water having Mediterranean sea origin. Other locations of this saltier pool can be thought about. But as it was already mentioned, we started from an initial state at rest where the denser water is likely to occupy the deepest part of the basin which is precisely located.

Finally, one could legitimately wonder whether a complex interplay between advection and diffusion processes could not lead to other sets of controls. Obviously enough, it results the same to diffuse slowly but during a sufficiently long time or to diffuse rapidly over a short duration. In our case, the vertical mixing localised above the salt pool is realised at once, before the implied water masses are advected (Figure 7). This allows to distinguish the two processes and to think that the

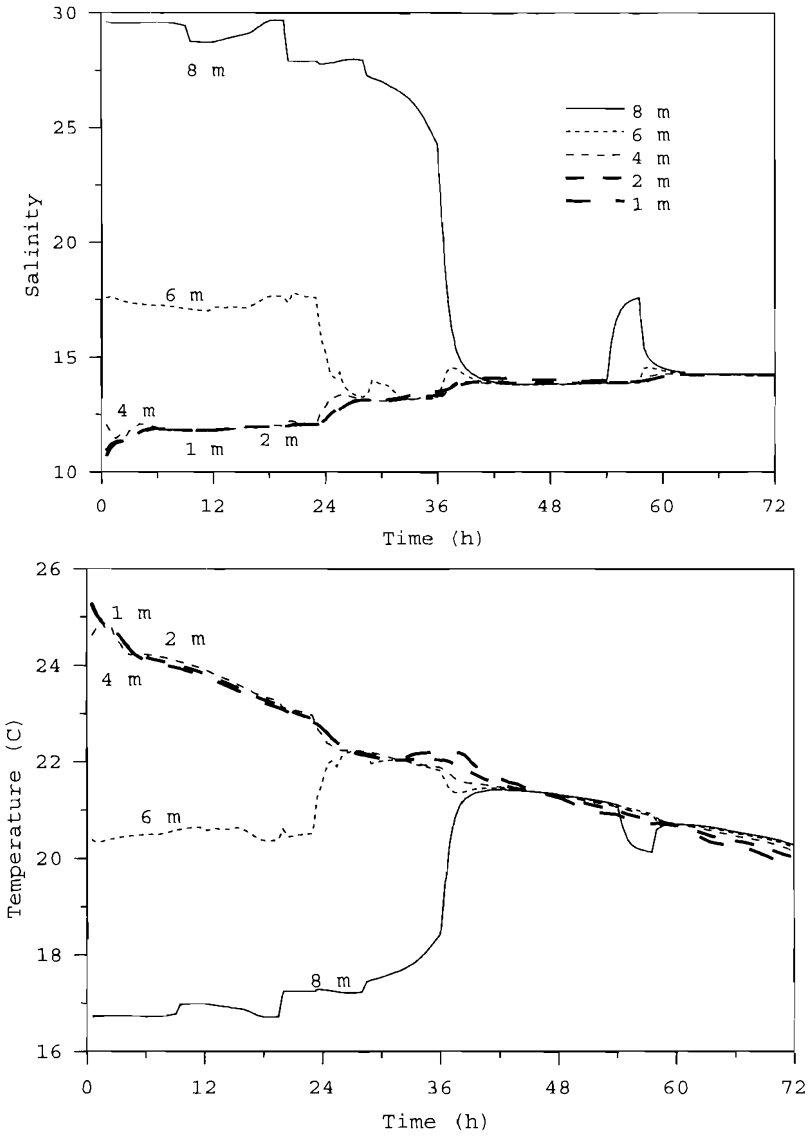

Figure 6. Salinity and temperature simulated by the optimised zero order model at the measurement station.

discrepancies between model results and data arise from an imperfect specification of the turbulent diffusivity coefficients. The preceding considerations show that the separation of advective and diffusive effects could not be generalised to other situations without cautions.

This optimisation of a vertical turbulent viscosity, which is assumed to be horizontally uniform, sets the problem of the relevance of the model results for the rest of the basin. At first sight, the results of the whole basin appear to be consistent. The full 4D fields representation being difficult, we have shown arbitrary features at t = 36 h, *i.e.* when the Mistral is the most intense, and the turbulent mixing is about to reach the entire water column down to 8 m depth. The surface current is strong and directed southwards. A return bottom current induces an advection of the deep marine water from the south to the north of the basin. Figure 9 shows the depth-integrated flow and the free surface elevation. The free surface slope along the wind direction is about 2 cm/km between the south and the north. As already observed on VHF radar surface current measurements, the flows along the east side are strong inducing significant biochemical and sedimentary transports. Figure 10 shows the horizontal variability of salinity and currents along a southeast north-west radial. In addition to the vertical mixing, a northwards advection of the salted marine water trapped in the deepest zone of the basin can be noticed.

Conclusion

The Berre lagoon hydrodynamics under strong north wind conditions was studied owing to a 3D primitive equations

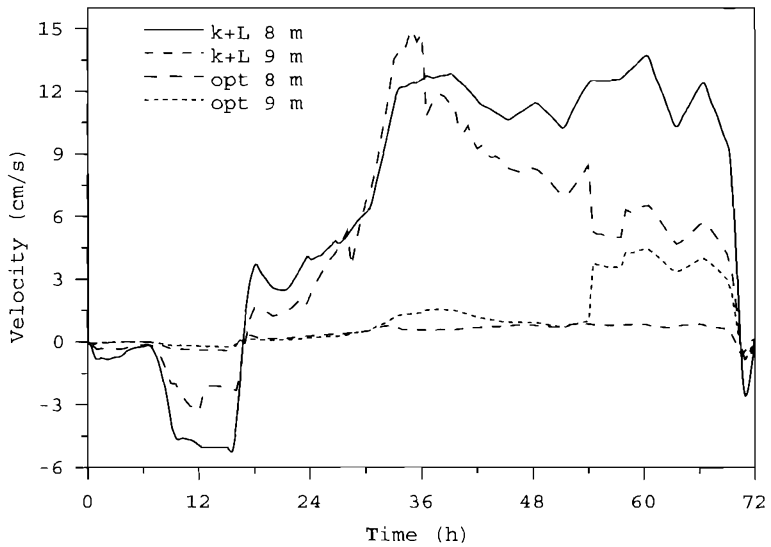

Figure 7. Bottom northward horizontal velocity, at 8 m and 9 m depth, 1 km Southeast from the measurement station, simulated by the k+L model and by the optimised zero order model.

model, assimilating T-S data to optimise the turbulent viscosity and diffusivities. The obtained optimal simulation is consistent with the physics of the model and is considered as the closest to the data.

The physical processes involved in the mixing of the fresh and marine waters were analysed. The wind induced mixing of the upper water column is baffled by the pycnocline acting as a wall. The turbulent energy remains trapped in this fresh upper layer until mechanical mixing energy overcomes the stabilising effects of the stratification. The pycnocline is then suddenly broken, the motion and the heat can diffuse downward, and the salinity, upward.

In addition to this vertical mixing, the 3D numerical model results give an insight of the subtle coupling between mixing and other phenomena such as the horizontal advection. For example, the marine waters stored in the south and the bottom of the basin are first vertically mixed and, after that, advected northwards. It is worthwhile to note that this particularity allows for this physical process to be correctly reproduced by the assimilation procedure.

The optimal control method has confirmed its ability to deal with a concrete problem of marine dynamics, even if further advances can be expected. First, numerical difficulties keep us from applying a 4-D space-time variational algorithm on the whole simulation period. A piecewise optimisation has been adopted giving already satisfactory results. Nevertheless, the optimal control of a sequence is deduced only from the data at the beginning and the end of the current sequence. A progress could be the optimisation of the control assimilating the data as a whole, taking into account the past

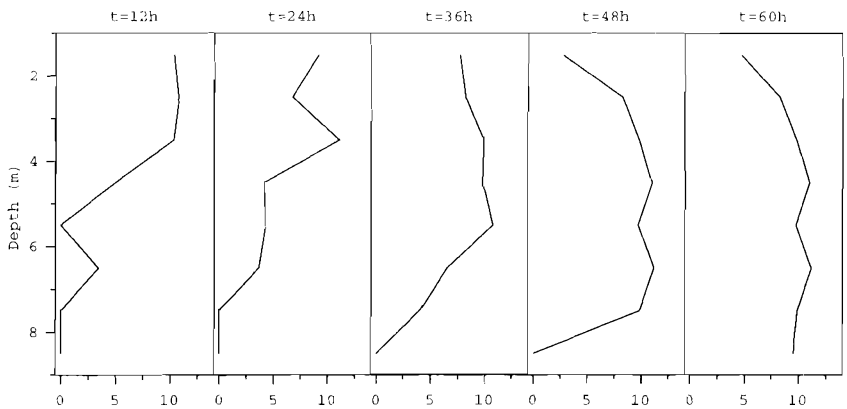

Figure 8. Vertical profiles of optimal turbulent viscosity ($cm^2 s^{-1}$).

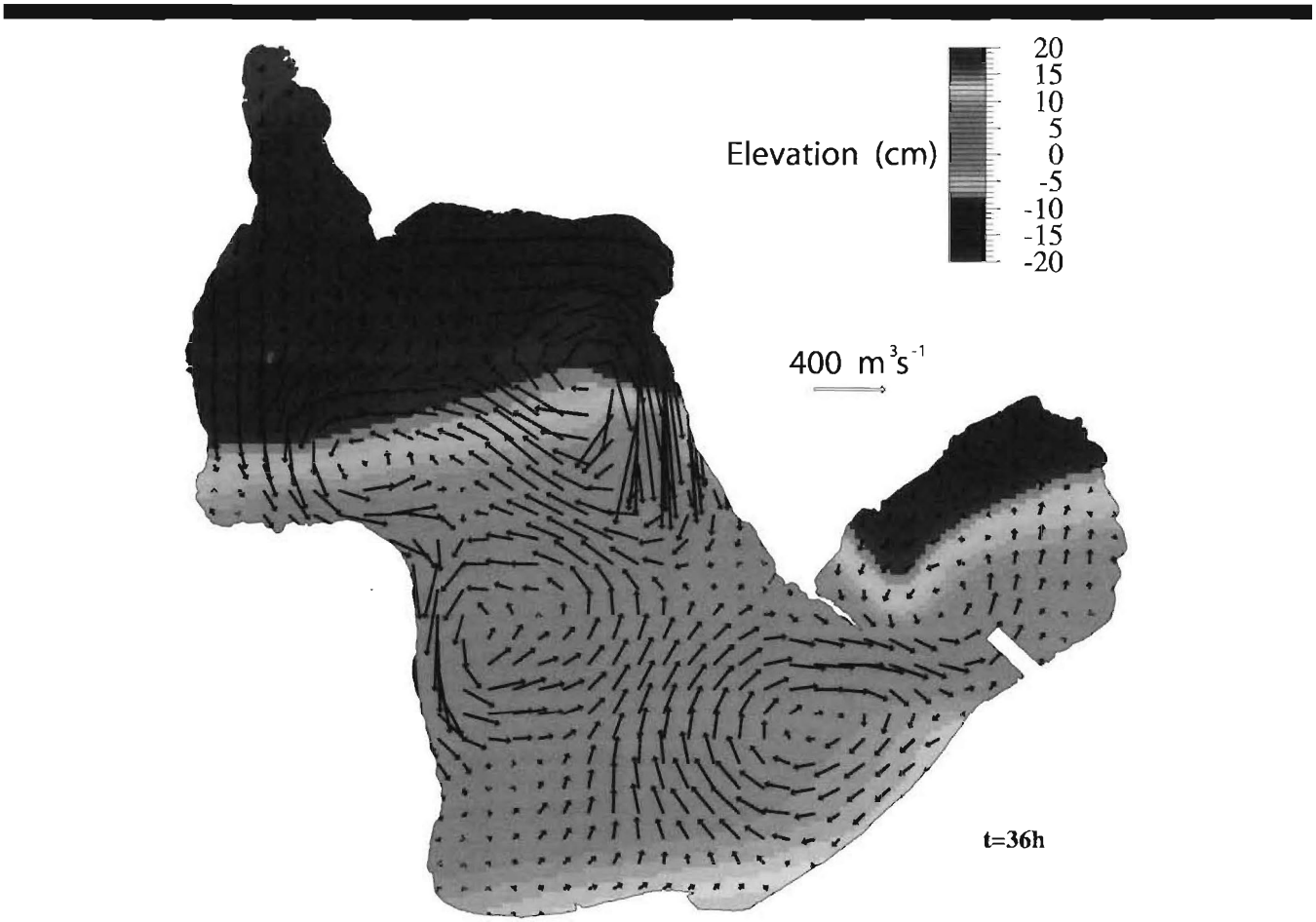

Figure 9. Free surface elevation (cm) and depth-integrated transport simulated by the optimised zero order model.

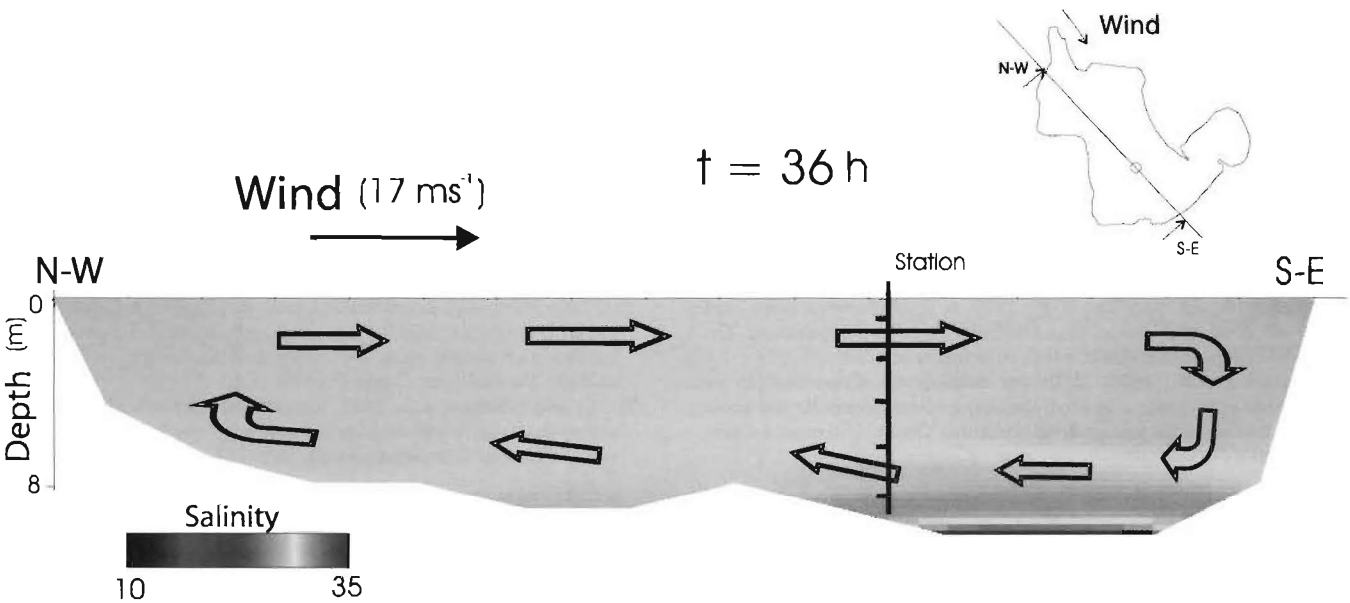

Figure 10. Salinity simulated by the optimised zero order model and schematic view of the associated circulation pattern along a South-East/North-West radial line at t = 36 h.

and future states. A 1D schematic example is given in LEREDDE *et al.* (1999).

Second, even if it seems that the zero order model assorted with turbulent viscosity optimisation gives qualitative satisfactory results for the whole basin, no quantitative assessments allow us to decide so. Taking an horizontally homogeneous viscosity field can seem to be a defective method. The zero order model with data assimilation allows us to reproduce closer the data at the measurements station location, but does not give enough physical consistency to extrapolate the results elsewhere in the basin. It would be necessary to ensure a better physical consistency for the viscosity field. A turbulence model, such as the k+L one, induces this physical consistency by setting additional constraints. In this kind of model, the turbulent viscosity and diffusivities and their corresponding simulation results will only depend upon a few number of modelling constants which can in turn be regarded as new model controls after which the optimal control method will seek. This last idea was illustrated in a prospective study on a schematic case (LEREDDE *et al.*, 2000).

ACKNOWLEDGEMENTS

We thank F. Garcia (Mission de Reconquête de l'Etang de Berre) and D. Nerini (Centre d'Océanologie de Marseille) for providing the T-S data.

LITERATURE CITED

BEGIS, D. and CREPON, M., 1975. On the generation of currents by winds: An identification method to determine oceanic parameters. *Lecture notes in Physics,* 58.

BLUMBERG, A. F. and GOODRICH, D. M. 1990. Modeling of wind-induced destratification in Chesapeake Bay. *Estuaries,* 13, 3, 236–249.

DEVENON, J. L., 1990. Optimal Control Theory Applied to an Objective Analysis of a Tidal Current Mapping by HF Radar. *Journal of Atmospheric and Oceanic Technology,* 7, 269–284.

EKNES, M. and EVENSEN, G., 1997. Parameter estimation solving a weak constraint variational formulation for an Ekman model. *Journal of Geophysical Research,* 102 (C6), 12, 479–491.

GILBERT, J.C. and LEMARECHAL, C., 1989. Some numerical experiments with variable-storage quasi-Newton algorithms. *Mathematical Programming,* 45, 407–435.

LE DIMET, F.X. and TALAGRAND, O., 1986. Variational algorithms for analysis and assimilation of meteorological observations: theoretical aspects. *Tellus,* 38A, 97–110.

LEENDERTSE, J.J.; ALEXANDER, R.C., and LIU, S.-K., 1973. A three-dimensional model for estuaries and coastal seas: Principles of computation. The RAND Corporation (California), internal report.

LEENDERTSE, J.J. and LIU, S.-K., 1977. A three-dimensional model for estuaries and coastal seas: Turbulent energy computation. The RAND Corporation (California), internal report.

LELLOUCHE, J.M., 1995. Méthodes numériques d'assimilation de données appliquées à la modélisation tridimensionnelle des écoulements en milieu peu profond. Doctoral Thesis. Université d'Aix-Marseille II, 162 pp.

LELLOUCHE, J.M.; DEVENON, J.L., and DEKEYSER, I., 1998. Data assimilation by optimal control in a 3-D coastal oceanic model: the problem of the discretization. *Journal of Atmospheric and Oceanic Technology,* 15, 2, 470–481.

LEREDDE, Y.; LELLOUCHE, J.M.; DEVENON, J.L., and DEKEYSER, I., 1998. On initial, boundary conditions and viscosity coefficient control for Burgers' equation. *International Journal of Numerical Methods in Fluids,* 28, 113–128.

LEREDDE, Y., 1999. Méthode d'assimilation de données par contrôle optimal appliquée à l'estimation de paramètres de diffusion turbulente dans un modlèle 3D de circulation océanique. Doctoral thesis. Université d'Aix-Marseille II. 149 pp.

LEREDDE, Y.; DEVENON, J.L., and DEKEYSER, I., 1999. Turbulent viscosity optimized by data assimilation. *Annales Geophysicae,* 17, 1463–1477.

LEREDDE, Y.; DEVENON, J.L., and DEKEYSER, I., 2000. Peut-on identifier les constantes d'un modèle de turbulence par assimilation d'observations, *Compte Rendus de l'Académie des Sciences,* 331, 405–412.

LIONS, J.L., 1968. *Contrôle optimal de systèmes gouvernés par de opérateurs aux dérivées partielles.* Dunod Eds., Paris, 426p.

MAROTZKE, J.; GIERING, R.; ZHANG, K.Q.; STAMMER, D.; HILL, C., and LEE, T., 1999. Construction of the adjoint MIT ocean circulation model and application to Atlantic heat transport sensitivity. *Journal of Geophysical Research,* 104 (C12) 29,529, 29,547.

MELLOR, G.L. and YAMADA, T., 1982. Development of a turbulence closure model for geophysical fluid problems. *Review of Geophysics Space and Physics,* 20, 851–875.

MOORE, A.M., 1991. Data assimilation in a quasi-geostrophic open-ocean model of the Gulf Stream region using the adjoint method. *Journal of Physical Oceanography,* 21, 398–427.

NERINI, D.; DURBEC, J.P., and MANTE, C., 2000. Analysis of oxygen rate time series in a strongly polluted lagoon using a regression tree method. *Ecological Modelling,* 133, 95–105.

NERINI, D.; DURBEC, J.P.; MANTE, C.; GARCIA, F., and GHATTAS, B., 2001. Forecasting physicochemical variables by a classification tree method. Application to the Berre lagoon (South France). *Acta biotheoretica,* in press.

NIHOUL, J.C.J., 1977. *Modèles mathématiques et dynamique de l'environnement.* Liège: ELE, 198p.

PANCHANG, V.G. and RICHARDSON, J.E., 1993. Inverse adjoint estimation of eddy viscosity for coastal flow models. *Journal of Hydraulic Engineering,* 119, 4, 506–524.

ROQUET, H.; PLANTON, S., and GASPAR, P., 1993. Determination of ocean surface heat fluxes by a variational method. *Journal Geophysical Research,* 98 (C6), 10, 211–221.

SCHILTZ, S.; RAIMBAULT, P., and MILLET, B., 2001. Eutrophication in Berre Lagoon: consequence of an organic matter storage in the sediment. *Comptes Rendus de l'Académie des Sciences,* submitted.

SEILER, U., 1993. Estimation of open boundary conditions with the adjoint method. *J. Geophys. Res.,* 98 (C12) 22,855–22,870.

THOUVENIN, B. and SALOMON, J.C., 1984. Modèle tridimensionnel de circulation et de dispersion en zone côtière à marée. Premiers essais: cas schématiques et baie de Seine. *Oceanol. Acta,* 7(4), 417–429.

VAN DAM, G.C. and LOUWERSHEIMER, R.A., 1990. A three-dimensional transport model for dissolved and suspended matter in estuaries and coastal seas. *Dynamics and Exchanges in Estuaries and the Coastal zone,* David Prandle (Ed.)

YU, L. and O'BRIEN, J.J., 1991. Variational estimation of the wind stress drag coefficient and the oceanic eddy viscosity profile. *Journal of Physical Oceanography,* 21, 709–719.

☐ Résumé ☐

L'Etang de Berre (France) est un bassin semi-ouvert de 6 m de profondeur moyenne et 155 km² de superficie. A cause de l'embouchure de la Durance au Nord et des intrusions d'eaux marines méditerranéennes au sud, la situation hydrologique est souvent fortement stratifiée. Le mélange vertical ne s'effectue qu'en cas de forts vents (> 10ms $^{-1}$).

La modélisation de la circulation du bassin durant un tel événement, avec un modèle 3D aux équations primitives, requiert une paramétrisation précise de la viscosité et des diffusivités verticales turbulentes. Une approche classique consiste à utiliser un modèle de turbulence tel que les modèles k-L ou k-ϵ. On propose ici une approche alternative qui consiste à considérer la viscosité ν_t, variable en espace et en temps, comme un paramètre de contrôle du systeme, en supposant des

nombres de Prandtl et Schmidt constants pour les diffusivités turbulentes. ν_t est optimisée de façon itérative pour chaque niveau et chaque période d'une demi-heure afin de minimiser l'écart entre les résultats de simulations et les profils de température et salinité mesurés par une station automatique toutes les demi-heures. Cette procédure itérative d'assimilation de données met en oeuvre un modèle adjoint.

La méthode du contrôle optimal est appliquée à une période de trois jours de vents et fournit des résultats de simulation plus proches des observations que ceux obtenus grâce à un modèle k + L classique sans assimilation de données.